OPEN ACCESS
IOP Publishing | ISECAEP
Journal of Reliability Science and Engineering
J. Reliab. Sci. Eng. **1** (2025) 025003 (19pp)
https://doi.org/10.1088/3050-2454/add161

AK-MCS structural reliability analysis method based on improved active learning function

Hongyan Chu[1,2], Wenzhong Li[1,2], Dongyang Sun[1,2], Zhifeng Liu[1,2,3], Weixu Zheng[1,2], Jingjing Xu[1,2,*] and Qiang Cheng[1,2]

[1] Institute of Advanced Manufacturing and Intelligent Technology, Beijing University of Technology, Beijing, People's Republic of China
[2] Beijing Key Laboratory of Design and Intelligent Machining Technology for High Precision Machine Tools, Beijing University of Technology, Beijing, People's Republic of China
[3] Key Laboratory of Advanced Manufacturing and Intelligent Technology for High-end CNC Equipment, Jilin University, Changchun, People's Republic of China

E-mail: xujj0908@bjut.edu.cn

Received 18 February 2025, revised 2 April 2025
Accepted for publication 27 April 2025
Published 15 May 2025

Abstract

In the field of engineering structural reliability analysis, there are often implicit and highly nonlinear performance function issues. When using approximate analytical methods to estimate failure probability, the resulting calculations typically involve significant errors. Although numerical simulation methods can provide high-accuracy solutions for failure probabilities, they are hindered by excessively long computation times. Consequently, reliability analysis methods based on active learning Kriging models have gained widespread application in the reliability analysis of engineering structures. This paper, based on the classical *U* learning function, comprehensively considers the impact of sample point prediction values and prediction variances on the accuracy of failure probability estimation. In the sample space, priority is given to selecting sample points that are closer to the limit state surface, and higher weights are assigned to the prediction variances of these sample points. Based on this, a *WU* learning function is proposed. In constructing the *WU* learning function, the appropriate adaptive orientation function is determined by comparing the sample selection effectiveness of the *WU* function under various adaptive orientation functions. Furthermore, the AK-MCS-WU reliability analysis method is introduced in conjunction with the Kriging model. Two numerical examples and one engineering case demonstrate that the proposed AK-MCS-WU method can ensure the stable convergence of failure probability, while providing efficient and accurate predictions of structural failure probability for reliability problems involving complex performance functions.

* Author to whom any correspondence should be addressed.

Keywords: structural reliability analysis, active learning function, Kriging surrogate model, adaptive orientation function

1. Introduction

The primary objective of structural reliability analysis is to calculate the probability of structural failure. In the analysis, the performance function $G(x)$ is used to represent the failure state of the structure: when $G(x) < 0$, the sample points lie within the failure domain; when $G(x) > 0$, the sample points are within the safe domain; and when $G(x) = 0$, the sample points lie on the limit state surface (LSS). Therefore, using the Monte Carlo simulation (MCS) method, the mathematical expression for calculating the failure probability of the structure is:

$$P_f = \int\limits_{G(x)\le 0} f_X(x)\,\mathrm{d}x = \int\limits_{R^n} I[G(x)] f_X(x)\,\mathrm{d}x = E_{\mathrm{f}}\{I[G(x)]\} \tag{1}$$

where $f_X(x)$ is the joint probability density function of random input variables, $E_f(\cdot)$ represents the mathematical expectation based on $f_X(x)$, and $I[G(x)]$ is the failure indicator function of the performance function. The mathematical definition of $I[G(x)]$ is:

$$I[G(x)] = \begin{cases} 1 & G(x) \le 0 \\ 0 & G(x) > 0 \end{cases}. \tag{2}$$

By converting the expectation in equation (1) into a summation, the unbiased estimate of P_{f} is:

$$\hat{P}_{\mathrm{f}} = \frac{1}{N_{\mathrm{MCS}}} \sum_{i=1}^{N_{\mathrm{MCS}}} I[G(x_i)] = \frac{N_{\mathrm{f}}}{N_{\mathrm{MCS}}} \tag{3}$$

where N_{MCS} is the number of sample points extracted from the random variables according to $f_X(x)$, and N_{f} is the number of failure sample points.

According to equation (3), the coefficient of variation of the structural failure probability is calculated as:

$$\mathrm{Cov}\left(\hat{P}_{\mathrm{f}}\right) = \sqrt{\frac{1-\hat{P}_{\mathrm{f}}}{(N_{\mathrm{MCS}}-1)\hat{P}_{\mathrm{f}}}}. \tag{4}$$

For practical engineering problems, directly calculating the structural failure probability through multiple integrals often presents significant challenges. To effectively compute the structural failure probability, many researchers have proposed a range of methods, primarily including approximate analytical methods, numerical simulation methods, and surrogate model methods. The approximate analytical methods mainly consist of the first-order reliability method [1, 2] and the second-order reliability method [3, 4], among others. In the context of numerical simulation, using MCS [5] to assess failure probability is a key technique in reliability analysis. When addressing reliability problems involving small failure probabilities, methods such as importance sampling (IS) [6, 7], subset simulation (SS) [8, 9], line sampling [10], and sequential space transformation [11] are commonly employed to predict the structural failure probability. Although numerical approximation methods are computationally efficient, ensuring solution accuracy becomes challenging when dealing with implicit and nonlinear function problems. On the other hand, while numerical simulation methods can provide highly accurate solutions for structural failure probabilities, they require extensive computational resources, limiting their practical applicability.

Surrogate model technology is one of the most widely used approaches in the current field of structural reliability research. Common surrogate models include polynomial chaos expansion [12], support vector machine models [13], radial basis function [14], neural network models [15], and Kriging models [16, 17], among others. Among these surrogate models, the Kriging model, based on Gaussian process regression, stands out. Compared to other surrogate models, the Kriging model offers unique advantages: it not only provides predicted values but also calculates the prediction variance for sample points, and the magnitude of this variance reflects the uncertainty of the predicted values.

The Kriging model was first proposed by Krige [18] for surveying the distribution of mineral resources. Later, French mathematician Matheron [19] extended and refined the model, forming a complete theoretical framework. Lophaven *et al* [20] developed the DACE toolbox on the MATLAB platform for constructing Kriging models, providing significant convenience for researchers worldwide and greatly promoting the widespread application of Kriging models in various fields. Kaymaz [21] was the first to introduce Kriging models into structural reliability analysis, using the DACE toolbox, and demonstrated the superiority of this approach. However, to achieve a Kriging model that meets accuracy requirements, a large number of initial sample points are typically required, leading to high computational costs. In response, many scholars have proposed a new reliability analysis method that combines surrogate models and sampling techniques through active learning. Notably, the active learning reliability analysis framework AK-MCS (Active learning reliability method combining Kriging and MCS) proposed by Echard *et al* [22] has received considerable attention. This method initially constructs a Kriging model using a small number of sample points and then selects the best iterative sample points through the active learning function, continuously refining the Kriging model until it meets the desired

accuracy, ultimately enabling precise failure probability prediction.

Recent improvements to the AK-MCS method focus primarily on two areas. First, various strategies and methods are integrated into the sampling process to enhance analysis efficiency. In particular, when dealing with small failure probability problems, the AK-MCS method often requires a significant number of iterations, leading to a sharp increase in computational effort, which can be impractical in engineering applications. To address this, Huang *et al* [23] replaced the MCS with SS in the AK-MCS method, resulting in the AK-SS method for small failure probability problems. Echard *et al* [24] introduced IS into the AK-MCS framework, forming the AK-IS reliability analysis method. Compared to AK-MCS, AK-IS improves computational efficiency by generating better candidate sample points through sampling techniques. Second, in adaptive structural reliability analysis based on Kriging models, the sample point selection strategy plays a crucial role in both model accuracy and computational efficiency. Several researchers have studied different point-selection methods, proposing various learning functions. Notably, the U function proposed by Echard *et al* [22], which considers the probability of misestimating the sign of sample points, and the expected feasibility function (EFF) proposed by Bichon *et al* [25], which accounts for sample points near the LSS with high variance, are representative examples. Additionally, Lv *et al* [26] proposed the H function, which uses information entropy to measure uncertainty around the LSS. The H learning function quantifies the Kriging model's fitting uncertainty near the limit state and selects sample points with the highest information entropy, thus enhancing computational efficiency. Zhu and Du [5] proposed a D learning function that considers the contribution of individual sample points to failure probability prediction errors and the correlation among all points, improving reliability analysis efficiency.

Other common learning functions include: Zhang *et al* [27] and Shi *et al* [28], who developed the reliability-based expected improvement function and folded normal-based expected improvement function, respectively, based on folded normal distributions; Yang *et al* [29], inspired by the 'Improved Expected Function', who proposed the risk expectation function, which measures the sign prediction accuracy of Kriging models; and Sun *et al* [30], who introduced a minimum improvement function that balances Kriging variance and joint probability density functions in failure probability estimation, effectively avoiding sample wastage in areas with small probability density values. The termination of the active learning process is determined by a convergence criterion. In this regard, Wang and Shafieezadeh [31] proposed an error-based convergence criterion, while Zhang *et al* [32] developed a new stopping criterion based on the expected upper limit of relative error in failure probability.

As a classical active learning function, many researchers have proposed improvements to the U function. Peijuan *et al* [33] added a line search step to the traditional U function, allowing the improved version to find training points closer to the limit state function than the original best points. Meng *et al* [34] introduced an improved U function, which sets acceptance and rejection domains for sampling points, effectively avoiding calculation waste caused by local sample point clustering, enhancing both efficiency and robustness in solving complex reliability problems. Cao *et al* [35] proposed the VF learning function by selecting candidate samples near the LSS and multiplying the Kriging model's prediction standard deviation by the probability density function.

In the process of selecting the best sample point, the U learning function defines it as the ratio of predicted mean to predicted variance. However, it does not consider the differing contributions of the predicted mean and variance to active learning. For instance, a sample point with a small predicted mean may not necessarily have a large predicted variance. To address this, this paper improves the traditional U function by proposing the WU active learning function, which assigns different weights to prediction variance based on Kriging's predicted mean. Compared to the U learning function, WU enhances failure probability prediction accuracy and reduces the number of performance function evaluations, thus improving analysis efficiency.

The structure of the remainder of this paper is as follows: section 2 briefly introduces the AK-MCS method, the Kriging model, and active learning functions. Section 3 elaborates on the construction process of the WU learning function, an improvement on the U function, and provides an analysis. Section 4 validates the advantages of the WU learning function through two numerical examples and one engineering example. Section 5 presents the conclusions of the study.

2. Structural reliability analysis method based on Kriging model

2.1. AK-MCS method

The core concept of the AK-MCS method lies in leveraging the Kriging model's ability to effectively approximate black-box functions. In engineering reliability problems, the Kriging surrogate model replaces the actual response function to perform reliability analysis. The implementation process involves combining the active learning function with the Kriging model. The active learning function is used to continuously select the optimal sample points for constructing the Kriging model, thereby iteratively improving the model. Once a Kriging model that meets the accuracy requirements is obtained, the MCS method is applied to predict the structural failure probability.

2.2. Kriging model

The Kriging model is an exact semi-parametric interpolation method. It uses spatial estimation techniques to perform a weighted linear combination of the surrounding information of the sample point in order to predict the value at that point. Not only does it provide the predicted mean for the point,

but it also offers the local prediction variance. Notably, the Kriging model's prediction error has a mean of zero, and its mean squared error is minimized, making it an optimal linear unbiased estimator.

The specific expression of the Kriging model is:

$$G(\boldsymbol{x}) = f^{\mathrm{T}}(\boldsymbol{x})\boldsymbol{\beta} + z(\boldsymbol{x}) \tag{5}$$

where x represents any input variable, G is the corresponding predicted response value, $f(\boldsymbol{x}) = [f_1(\boldsymbol{x}), f_2(\boldsymbol{x}), \cdots, f_m(\boldsymbol{x})]^{\mathrm{T}}$ is the vector of basis functions for the polynomial, m is the number of polynomials, and $\boldsymbol{\beta} = [\beta_1, \beta_2, \cdots, \beta_m]^{\mathrm{T}}$ is the vector of regression coefficients. $f^{\mathrm{T}}(\boldsymbol{x})\boldsymbol{\beta}$ represents a parameterized polynomial model that captures the trend in the Kriging model. The stochastic process $z(\boldsymbol{x})$ follows a Gaussian distribution $N(0, \sigma^2)$ and provides a local approximation of Kriging's simulation. The covariance equation between any two sample points x_i and x_j in the sample set can be expressed as:

$$\mathrm{Cov}[z(\boldsymbol{x}_i), z(\boldsymbol{x}_j)] = \sigma^2 R(\theta, \boldsymbol{x}_i, \boldsymbol{x}_j) \tag{6}$$

where $R(\theta, \boldsymbol{x}_i, \boldsymbol{x}_j)$ is the correlation function that represents the spatial correlation between the sample points $\boldsymbol{x}_i$ and $\boldsymbol{x}_j$, and $\theta = [\theta_1, \theta_2, \cdots, \theta_n]^{\mathrm{T}}$ is vector of correlation parameters. The typical correlation function used is the Gaussian correlation function, and its specific form is:

$$R(\theta, \boldsymbol{x}_i, \boldsymbol{x}_j) = \prod_{m=1}^{M} \exp\left[-\theta_m \left(\boldsymbol{x}_i^m - \boldsymbol{x}_j^m\right)^2\right] \tag{7}$$

where x_i^m and x_j^m represent the mth element of x_i and x_j respectively, and θ_m is the correlation parameter corresponding to the mth directional component. This parameter represents the relationship between the distance and the degree of correlation among design sample points, and its magnitude directly influences the prediction results of the Kriging model.

given e initial sample points $X = [x_1, x_2, \cdots, x_e]$ and the corresponding true limit state function response values $G = [G(x_1), G(x_2), \cdots, G(x_e)]$, for the given correlation parameter $\theta = [\theta_1, \theta_2, \cdots, \theta_n]^{\mathrm{T}}$, the estimated values of the regression coefficients $\boldsymbol{\beta}$ and the variance of the Gaussian process are respectively:

$$\hat{\beta} = \left(\boldsymbol{F}^{\mathrm{T}}\boldsymbol{R}^{-1}\boldsymbol{F}\right)^{-1}\boldsymbol{F}^{\mathrm{T}}\boldsymbol{R}^{-1}\boldsymbol{G} \tag{8}$$

$$\hat{\sigma}^2 = \frac{1}{e}\left(\boldsymbol{G} - \boldsymbol{F}\hat{\boldsymbol{\beta}}\right)^{\mathrm{T}}\boldsymbol{R}^{-1}\left(\boldsymbol{Y} - \boldsymbol{F}\hat{\boldsymbol{\beta}}\right) \tag{9}$$

where $\widehat{\boldsymbol{\beta}}$ is the estimated polynomial parameter vector, $\hat{\sigma}^2$ is the estimate of variance σ^2, and $\boldsymbol{R}$ is the correlation coefficient matrix, with $\boldsymbol{R} = [R_{ij}]_{e\times e}$, where $R_{ij} = R(\theta, \boldsymbol{x}_i, \boldsymbol{x}_j)$ ..

The mean and variance of the Kriging prediction at a certain point x are:

$$\mu_{\hat{G}}(x) = \hat{G}(x) = \boldsymbol{f}^{\mathrm{T}}(x)\hat{\boldsymbol{\beta}} + \boldsymbol{r}^{\mathrm{T}}(x)\boldsymbol{R}^{-1}\left(\boldsymbol{G} - \boldsymbol{F}\hat{\boldsymbol{\beta}}\right) \tag{10}$$

$$\hat{\sigma}^2_{\hat{G}}(x) = \hat{\sigma}^2\left[1 + \boldsymbol{u}^{\mathrm{T}}(x)\left(\boldsymbol{F}^{\mathrm{T}}\boldsymbol{R}^{-1}\boldsymbol{F}\right)^{-1}\boldsymbol{u}(x) - \boldsymbol{r}^{\mathrm{T}}(x)\boldsymbol{R}^{-1}\boldsymbol{r}(x)\right] \tag{11}$$

where:

$$\boldsymbol{r}(\boldsymbol{x}) = [R(\theta, x_1, x), R(\theta, x_2, x), \cdots, R(\theta, x_e, x)] \tag{12}$$

$$\boldsymbol{u}(x) = \boldsymbol{F}^{\mathrm{T}}\boldsymbol{R}^{-1}\boldsymbol{r}(x) - \boldsymbol{f}(x). \tag{13}$$

The Kriging variance $\hat{\sigma}^2$ characterizes the prediction error at the point x, and its magnitude reflects the degree of uncertainty in the predicted value. This is a key basis for active learning methods.

2.3. Active learning function

(1) U learning function

Echard *et al* [22] proposed using the U learning function to select updated sample points. The U function is defined as follows:

$$U(x) = \frac{\left|\mu_{\hat{G}}(x)\right|}{\sigma_{\hat{G}}(x)} \tag{14}$$

where $\mu_{\hat{G}}(x)$ and $\sigma_{\hat{G}}(x)$ represent the predicted mean and predicted standard deviation of Kriging model at the sample points, respectively.

When the absolute value of the predicted mean $\mu_{\hat{G}}(x)$ is decreases, the corresponding U value also becomes smaller, indicating that the candidate sample point is closer to the limit state function; Moreover, a smaller U value corresponds to a larger Kriging prediction variance, which suggests higher prediction uncertainty at that sample point. In other words, this sample point is not only near the LSS but also has a higher Kriging prediction uncertainty.

Based on the above analysis, the optimal sample point should be the one corresponding to the minimum value of the formula. The specific point-selection method is as follows:

$$x_{\mathrm{new}} = \arg\min_{x\in S} U(x) \tag{15}$$

where x_{new} represents the optimal sample point, and S is the set of candidate points for the optimal sample.

The stopping criterion for the U learning function is $\min\{U(x) \geq 2\}$. At this point, the probability that the signs of the sample points in S are predicted correctly is at least $\Phi(2) = 97.7\%$, indicating that the Kriging model is sufficiently accurate.

(2) EFF learning function

Bichon *et al* [25] proposed the EFF, which is a function of both the predicted mean and predicted variance. The EFF function reflects how far the true response value is from the LSS $G(x) = b$. Its specific expression is as follows:

$$\begin{aligned}\mathrm{EFF}(x) = &\left(\mu_{\widehat{G}}(x) - b\right)\left[2\Phi\left(\frac{b-\mu_{\widehat{G}}(x)}{\sigma_{\widehat{G}}(x)}\right) - \Phi\left(\frac{(b-\varepsilon)-\mu_{\widehat{G}}(x)}{\sigma_{\widehat{G}}(x)}\right) - \Phi\left(\frac{(b+\varepsilon)-\mu_{\widehat{G}}(x)}{\sigma_{\widehat{G}}(x)}\right)\right] \\ &- \sigma_{\widehat{G}}(x)\left[2\phi\left(\frac{b-\mu_{\widehat{G}}(x)}{\sigma_{\widehat{G}}(x)}\right) - \phi\left(\frac{(b-\varepsilon)-\mu_{\widehat{G}}(x)}{\sigma_{\widehat{G}}(x)}\right) - \phi\left(\frac{(b+\varepsilon)-\mu_{\widehat{G}}(x)}{\sigma_{\widehat{G}}(x)}\right)\right] \\ &+ \varepsilon\left[\Phi\left(\frac{(b+\varepsilon)-\mu_{\widehat{G}}(x)}{\sigma_{\widehat{G}}(x)}\right) - \Phi\left(\frac{(b-\varepsilon)-\mu_{\widehat{G}}(x)}{\sigma_{\widehat{G}}(x)}\right)\right] \end{aligned} \tag{16}$$

where $\Phi(\cdot)$ is the standard normal distribution function; $\phi(\cdot)$ is the standard normal probability density function; $\varepsilon = 2\sigma^2_{\widehat{G}}(x)$; $b = 0$ represents the LSS.

The expression for the EFF function to select the best sample point is:

$$x_{\mathrm{new}} = \arg\max_{x\in S}\mathrm{EFF}(x). \tag{17}$$

The convergence criterion of the EFF function is:

$$\max\{\mathrm{EFF}(x)\} \le 10^{-3} \tag{18}$$

(3) H learning function

Based on information entropy theory, Lv *et al* [26] proposed the H learning function, with its specific expression given as follows:

$$H(x) = \left|\begin{array}{l}\ln\left(\sqrt{2\pi}\sigma_{\widehat{G}}(x) + \frac{1}{2}\right)\left[\Phi\left(\frac{2\sigma_{\widehat{G}}(x)-\mu_{\widehat{G}}(x)}{\sigma_{\widehat{G}}(x)}\right) - \Phi\left(\frac{-2\sigma_{\widehat{G}}(x)-\mu_{\widehat{G}}(x)}{\sigma_{\widehat{G}}(x)}\right)\right] \\ -\frac{2\sigma_{\widehat{G}}(x)-\mu_{\widehat{G}}(x)}{2}\phi\left(\frac{2\sigma_{\widehat{G}}(x)-\mu_{\widehat{G}}(x)}{\sigma_{\widehat{G}}(x)}\right) \\ +\frac{-2\sigma_{\widehat{G}}(x)-\mu_{\widehat{G}}(x)}{2}\phi\left(\frac{-2\sigma_{\widehat{G}}(x)-\mu_{\widehat{G}}(x)}{\sigma_{\widehat{G}}(x)}\right)\end{array}\right|. \tag{19}$$

The expression for the H function to select the best sample point is:

$$x_{\mathrm{new}} = \arg\max_{x\in S}H(x). \tag{20}$$

In this paper, the convergence criterion of the H function is set as:

$$\max\{H(x)\} \le 0.5. \tag{21}$$

3. Structural reliability analysis based on AK-MCS-WU method

The active learning function plays a crucial role in the AK-MCS method, with its performance directly influencing the fitting accuracy of the Kriging model and the number of evaluations of the performance function. In this section, a new WU learning function is proposed based on the U learning function. Compared to the U learning function, the WU learning function not only enhances the accuracy of the Kriging model but also reduces the number of performance function calls, thereby improving analysis efficiency.

3.1. WU learning function

According to the point-selection strategy of the U learning function, when selecting the best sample point, those with smaller predicted means and higher prediction variances are preferred. While the U learning function considers both the predicted values and prediction variances of sample points, for points in the sample set, even if a sample point is closer to the LSS (i.e. its predicted value is smaller), the prediction variance at that point may not necessarily be larger. Since both the predicted value and prediction variance of sample points influence the accuracy of failure probability estimation, it is preferable to prioritize sample points closer to the LSS. Additionally, a higher weight is assigned to the prediction variance of sample points near the LSS. Based on this, the WU learning function is proposed:

$$WU(x) = \frac{|\mu_{\widehat{G}}(x)|}{W(x)} \tag{22}$$

where $\mu_{\widehat{G}}(x)$ is the absolute value of the Kriging model's predicted mean, $W(x)$ is the adaptive weight function, and its expression is:

$$W(x) = \rho(x)\sigma_{\widehat{G}}(x) \tag{23}$$

where $\rho(x)$ is the adaptive orientation function, and $\sigma_{\hat{G}}(x)$ is the standard deviation of the Kriging model's sample predictions.

Building on the above analysis, the adaptive orientation function $\rho(x)$ should yield a higher value as the independent variable approaches 0. Based on the properties of the exponential function and the normal distribution probability density function, this paper provides two forms of $\rho(x)$ to address this requirement.

$$\rho_1(x) = 1 + \frac{5}{2\sqrt{2\pi}} \exp\left(-\frac{|\mu_{\hat{G}}(x)|^2}{2}\right) \tag{24}$$

$$\rho_2(x) = 1 + \exp\left(-\left|\mu_{\hat{G}}(x)\right|\right). \tag{25}$$

The data characteristics of the two adaptive orientation functions are analyzed individually, and the results are presented in figure 1. It can be observed from the figure that as $|\mu_{\hat{G}}(x)|$ approaches zero and becomes smaller, both adaptive orientation functions tend to converge towards a value of 2. Conversely, as $|\mu_{\hat{G}}(x)|$ increases, the values of these functions decrease. In comparison to $\rho_1(x)$, when $|\mu_{\hat{G}}(x)|$ is close to zero, function $\rho_2(x)$ exhibits a more pronounced change in its values, indicating a difference in steepness between the two functions. According to the weight distribution method of the *WU* learning function and considering the impact of sample point prediction variance, greater weights are assigned to sample points that are closer to the LSS.

Similar to the *U* function, the sample point corresponding to the minimum value of $WU(x)$ is considered the optimal sample point in the current Kriging model.

$$x_{\text{new}} = \arg\min\left[WU(x)\right]. \tag{26}$$

When the *WU* learning function stops active learning, the value of $|\mu_{\hat{G}}(x)|$ approaches 0, at which point $\rho(x) = 2$. Therefore, the *WU* learning function is related to the *U* learning function as follows:

$$WU(x) = \frac{\left|\mu_{\hat{G}}(x)\right|}{\rho(x)\sigma_{\hat{G}}(x)} = \frac{\left|\mu_{\hat{G}}(x)\right|}{2\sigma_{\hat{G}}(x)} = \frac{1}{2}U(x). \tag{27}$$

The stopping criterion for the *U* learning function is $\min\{U(x) \geq 2\}$. Based on this, the stopping criterion for the *WU* learning function can be derived as follows:

$$\min\{WU(x) \geq 1\}. \tag{28}$$

The effectiveness of the *U* learning function, *WU* learning function, and *WU* learning function under different adaptive orientation functions for sample point selection was compared. The simple function $G(x) = x_1^2 + x_2^2 - 16$ was analyzed and calculated to obtain the distribution of sample points selected by various learning functions, as shown in figure 2.

Comparing figure 2(a) with figures 2(b) and (c), the *U* learning function tends to select sample points that are farther from the LSS. In contrast, the *WU* learning function selects more sample points near the LSS, resulting in a lower overall number of selected sample points and, consequently, fewer calls to the performance function.

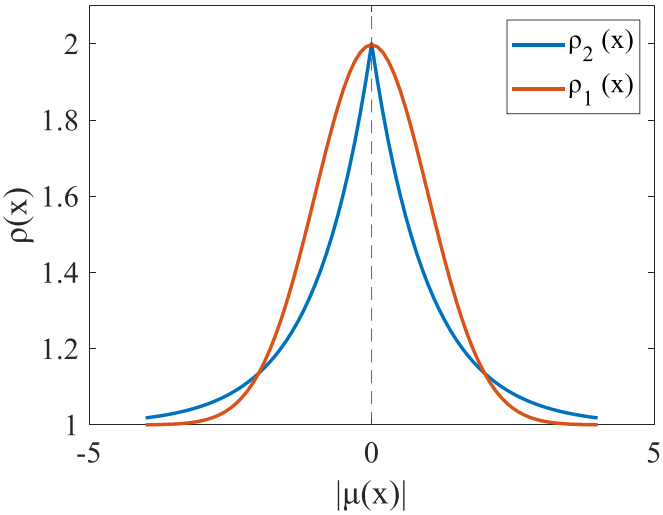

Figure 1. The adaptive orient function.

By further comparing figures 2(b) and (c), it is evident that the effectiveness of the *WU* learning function in selecting sample points varies depending on the choice of the adaptive orientation function. When using the adaptive orientation function $\rho_2(x)$, more sample points are located near the LSS, indicating that $\rho_2(x)$ leads to a more effective sample selection process for the *WU* learning function.

As analyzed earlier, compared to $\rho_1(x)$, $\rho_2(x)$ exhibits a steeper curve, with more pronounced changes in function values when $|\mu_{\hat{G}}(x)|$ is small and approaches zero. To further determine the parameters of the adaptive orientation function $\rho_2(x)$, two parameterized forms, $\rho_{2-1}(x)$ and $\rho_{2-2}(x)$ are introduced. The corresponding function curves are shown in figure 3. When using $\rho_{2-1}(x)$ and $\rho_{2-2}(x)$ as the adaptive orientation functions, the stopping criterion for the *WU* function is set as $\min\{WU(x) \geq 2/3\}$.

$$\rho_{2-1}(x) = 2 + \exp\left(-|\mu_{\hat{G}}(x)|\right) \tag{29}$$

$$\rho_{2-2}(x) = 1 + 2\exp\left(-\left|\mu_{\hat{G}}(x)\right|\right) \tag{30}$$

The effectiveness of the *WU* learning function corresponding to adaptive orientation functions with three different parameter settings in selecting sample points is compared, and the results are illustrated in figure 4. As shown in the figure, the sample points selected by the *WU* learning functions associated with these three parameterized adaptive orientation functions are all concentrated near the LSS, suggesting that their selection performance is comparable. Based on this analysis, $\rho_2(x)$ is ultimately chosen as the adaptive orientation function, leading to the final expression of the *WU* learning function.

$$WU(x) = \frac{|\mu_{\hat{G}}(x)|}{\left(1 + \exp\left(-|\mu_{\hat{G}}(x)|\right)\right)\sigma_{\hat{G}}(x)}. \tag{31}$$

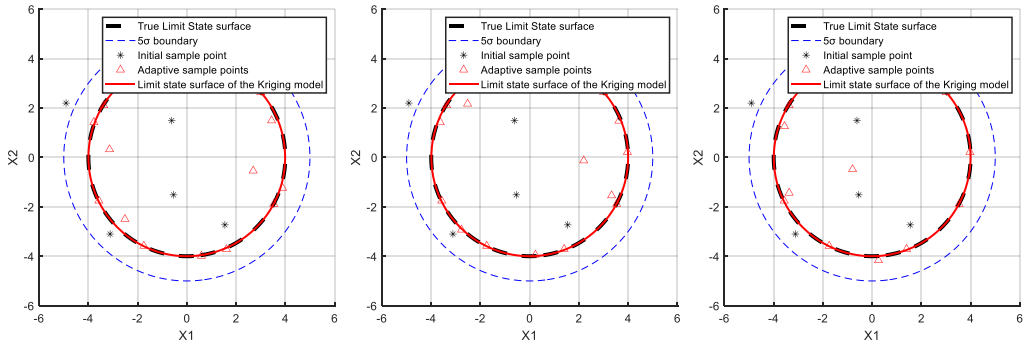

a) U learning function b) WU learning function(ρ_1) c) WU learning function(ρ_2)

Figure 2. Sample points selected by *U* and *WU*.

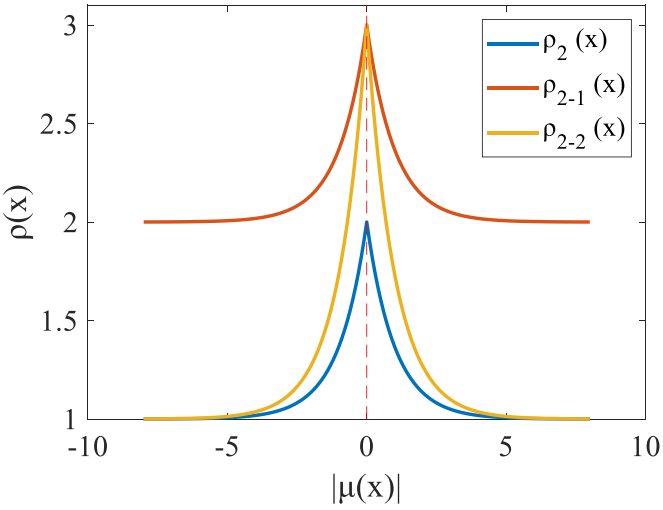

Figure 3. $\rho_2(x)$ with different parameters.

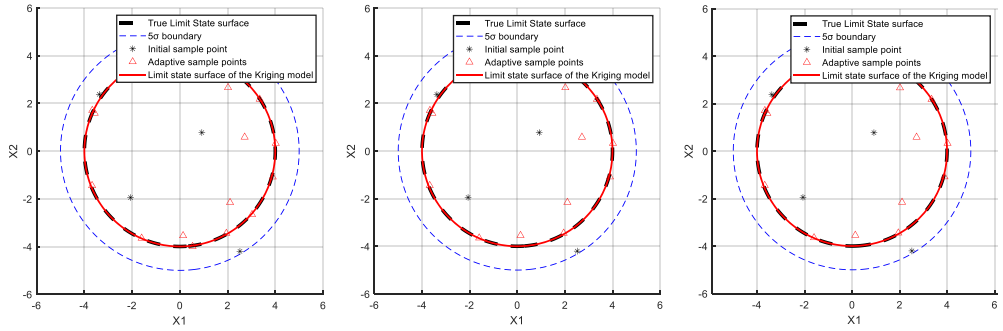

a) WU learning function(ρ_2) b) WU learning function($\rho_{2\text{-}1}$) c) WU learning function($\rho_{2\text{-}2}$)

Figure 4. Sample points selected by different *WU*.

3.2. Structural reliability analysis process based on AK-MCS-WU method

The present paper proposes a structural reliability analysis method based on the AK-MCS-WU approach. The key steps are outlined as follows.

Step 1: The MCS sample set N_{MCS} was established by employing Latin hypercube sampling to extract input samples of group m, based on the data characteristics of random input variables.

Step 2: The design of the experiment (DoE) was conducted. n initial sample points were selected from the sample set N_{MCS}, and the true response of these sample points was calculated and denoted as G.

Step 3: Utilizing the initial sample point and corresponding response value G, the DACE toolbox in MATLAB is employed to develop or refine the Kriging agent model.

Step 4: Based on the Kriging model, the predicted values for the N_{MCS} sample points are computed.

Step 5: Based on the *WU* learning function, the active learning function is calculated and the optimal sample point X^{new} is selected.

Step 6: Refine the learning function of *WU* and verify its convergence. If $\min\{WU(x \geq 1)\}$, proceed to Step 7. Otherwise, compute the response value G^{new} for X^{new}, update the DoE sample point set, and then advance to Step 3.

Step 7: Refine the coefficient of variation for the failure probability. Should the $\mathrm{Cov}(P_{\mathrm{f}}) \geq 0.05$, it is imperative to generate a novel initial candidate sample point and to augment the existing array of initial sample points. Subsequently, proceed to Step 2 anew. Conversely, if $\mathrm{Cov}(P_{\mathrm{f}}) < 0.05$, it will be concluded that the estimated failure probability is satisfactory, thereby achieving the final Kriging model and obtaining the structural failure probability.

The flow chart illustrating the AK-MCS-WU method is depicted in figure 5.

4. The experimental example verifies

In this section, the effectiveness of the proposed AK-MCS-WU method is validated through three case studies. All calculation results presented in this paper represent the average values obtained from ten independent random trials.Using the failure probability computed by the MCS method as a benchmark, the accuracy of each method is assessed, and the relative error for each method is calculated as follows:

$$\varepsilon_{\mathrm{error}} = \frac{\left| P_{\mathrm{f}}^{\mathrm{MCS}} - \hat{P}_{\mathrm{f}} \right|}{P_{\mathrm{f}}^{\mathrm{MCS}}} \times 100\% \tag{32}$$

where $P_{\mathrm{f}}^{\mathrm{MCS}}$ is the failure probability calculated by MCS method, and $\hat{P}_{\mathrm{f}}$ is the failure probability predicted by Kriging model.

4.1. Example 1: two-dimensional four-branch series system

The random variables x_1 and x_2 are independent and follow a standard normal distribution. The constant k is used to control the failure probability of the series failure system, with values of 6 or 7. The corresponding limit state function is defined as follows.

$$G(X) = \min \begin{Bmatrix} 3 + \dfrac{(x_1 - x_2)^2}{10} - \dfrac{(x_1 + x_2)}{\sqrt{2}} \\ 3 + \dfrac{(x_1 - x_2)^2}{10} + \dfrac{(x_1 + x_2)}{\sqrt{2}} \\ (x_1 - x_2) + \dfrac{k}{\sqrt{2}} \\ (x_2 - x_1) + \dfrac{k}{\sqrt{2}} \end{Bmatrix}. \tag{33}$$

In the sample space $[-5, +5]$ of the basic variables x_1 and x_2, use the Latin hypercube sampling to extract $N = 12$ initial sample points for DoE, and the number of initial sample points for MCS is $N_{\mathrm{MCS}} = 10^6$. The modeling results of the AK-MCS method based on the *WU* learning function proposed in this paper and several other common learning functions are shown in figures 6 and 7. The figures include the initial sample points, the updated sample points selected by the active learning function, the true limit state function, and the Kriging model.

It can be seen from figures 6 and 7 that the AK-MCS methods using different learning functions are all capable of fitting the true limit state function. Among them, the AK-MCS-EFF method, which employs the EFF learning function, selects the fewest best sample points, thereby minimizing the number of calls to the performance function. In comparison to the AK-MCS-U method, the AK-MCS-WU method has a distinct advantage in reducing the number of performance function evaluations. Additionally, the best sample points selected by the *WU* learning function are more concentrated near the limit state curve, which is conducive to improving the accuracy of the Kriging model and thus improving the prediction accuracy of the failure probability. In a certain test, the convergence curves of the failure probability and the relative—error curves of the evaluation results during the active learning process of various methods are shown in figures 8 and 9.

It can be seen from figures 8 and 9 that all methods can meet certain evaluation results. During the entire calculation process, the methods are sorted in ascending order of the number of iterations as AK-MCS-EFF, AK-MCS-H, AK-MCS-WU, and AK-MCS-U. Although the first two methods have fewer iterations, their relative errors in predicting the failure probability are relatively large. It can be seen from figures 8(b) and 9(b) that compared with the AK-MCS-U method, the AK-MCS-WU method has a larger prediction error in the initial stage of iteration. However, as the accuracy of the Kriging model continuously improves, the prediction error becomes

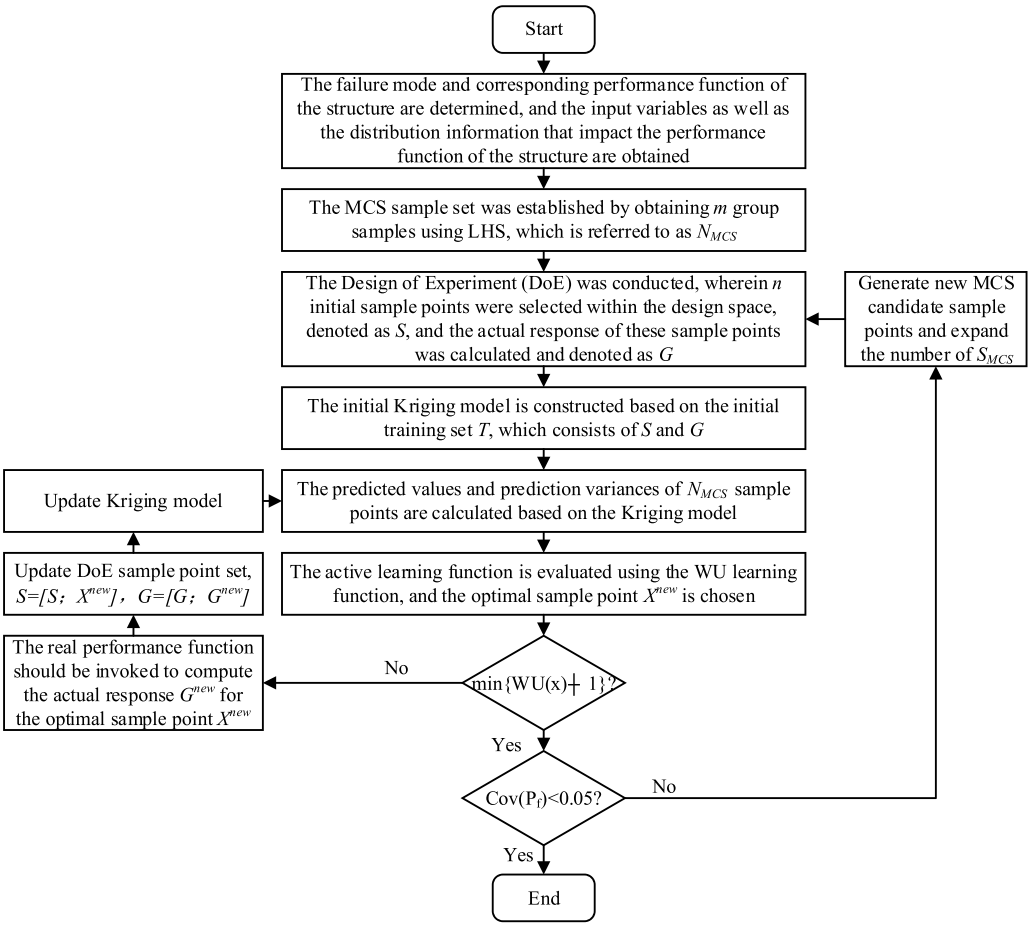

Figure 5. AK-MCS-WU method flow chart.

smaller and smaller, and finally, a Kriging model that meets the accuracy requirements is obtained.

The specific reliability calculation results of each method are shown in table 1. In the table, N_{call} represents the number of calls to the performance function, P_{f} represents the failure probability, $\text{Cov}_{P_{\text{f}}}$ represents the coefficient of variation, $\varepsilon_{\text{error}}$ is the relative error between the estimated value of the failure probability and the standard value, and T represents the solution time in seconds.

It can be seen from table 1 that when $k = 6$, the failure probability calculated by the MCS method is 4.473×10^{-3}, with the number of calls to the performance function is 1×10^{6}. The failure probability calculated by the AK-MCS-U method is 4.437×10^{-3}, with a relative error of 0.80%. Compared with the MCS method, the number of calls to the performance function of the AK-MCS-U method is significantly reduced, totaling 12 + 59.3 calls, where 12 represents the number of initial sample points and 59.3 represents the average number of performance function calls during the Kriging model reconstruction. The failure probability calculated by the AK-MCS-WU method is 4.500×10^{-3}, with a relative error of 0.60%, and the number of calls to the performance function is only 12 + 51.1 times. The average time required for the program to solve once is 143.83 s. The AK-MCS-EFF and AK-MCS-H methods result in 12 + 14.2 and 12 + 32.8 calls to the performance function, respectively, with prediction relative errors of 4.7% and 4.5%, and average solution times of 638.89 s and 688.21 s, respectively. When $k = 7$, all methods have similar effects on the estimation of the failure probability and the number of calls to the performance function.

In summary, although the AK-MCS-EFF method and the AK-MCS-H method can significantly reduce the number of calls to the performance function, their prediction accuracy is relatively low, and the average time required for each program run is quite long, resulting in high computational costs. Compared with the AK-MCS-U method, the AK-MCS-WU method can improve the accuracy of the failure probability estimation to a certain extent, reduce the number of calls to the performance function, and improve the efficiency of structural reliability analysis. In addition, the box plots of the number of calls to the real performance function by various methods are shown in figure 10.

It can be seen from figure 10 that compared with the AK-MCS-U method, the AK-MCS-WU method has a lower median number of calls to the performance function, and its box plot has a smaller box, which means that the AK-MCS-WU method has higher stability in the number

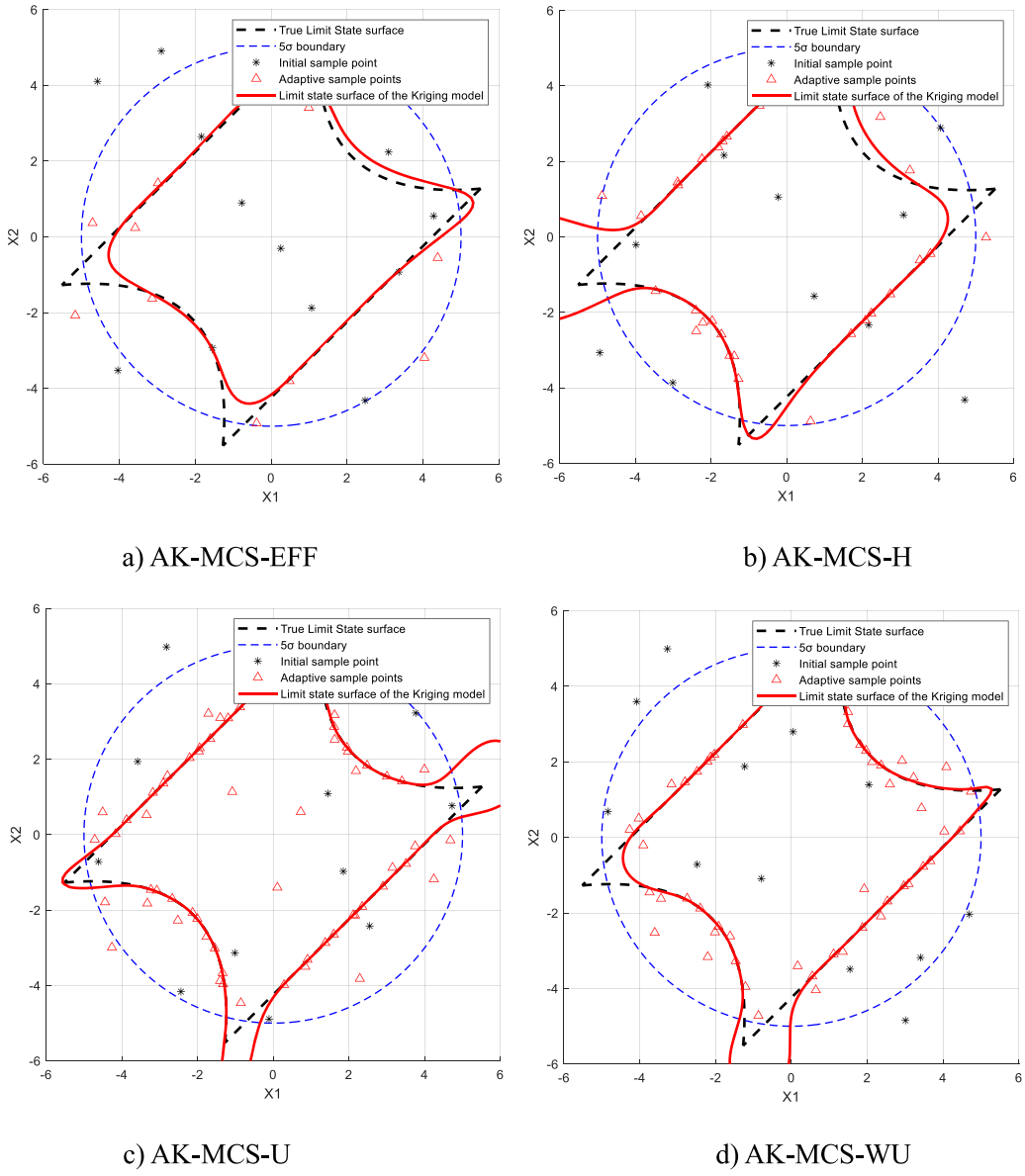

Figure 6. Modeling results of various methods when $k = 6$.

of calls to the performance function during the calculation process.

4.2. Example 2: nonlinear oscillator system

The figure 11 illustrates a widely utilized nonlinear oscillator for validating the reliability analysis method, with its corresponding performance function as fellow.

$$G(x) = 3r - \left|\frac{2F_1}{m\omega_0^2}\sin\left(\frac{\omega_0 t_1}{2}\right)\right| \tag{34}$$

where $\omega_0 = \sqrt{(c_1 + c_2)/m}$。
where c_1 and c_2 represents the spring stiffness, m denotes the car mass, and r signifies the given threshold.

The parameters of each random variable are presented in table 2. The random variables c_1, c_2, r, m, t and $F(t)$ are all independent and follow a normal distribution.

A Kriging model is constructed in the sample space $[-2, +2]$. The Latin hypercube sampling is used to extract $N = 12$ initial sample points for DoE, and the number of initial sample points for MCS is $N_{\mathrm{MCS}} = 10^6$. The reliability calculation results of the AK-MCS method based on the *WU* learning function proposed in this paper and several other common learning functions are shown in table 3.

The calculation results show that the AK-MCS-EFF method requires the fewest calls to the performance function but has the largest relative error. The number of calls to the performance function and the relative errors for the other three methods are similar. However, the AK-MCS-H method has the longest average solution time per run, at 130.72 s. Compared to the AK-MCS-U method, the AK-MCS-WU method reduces the number of calls to the performance function to some extent while achieving the smallest relative error in estimating the failure probability.

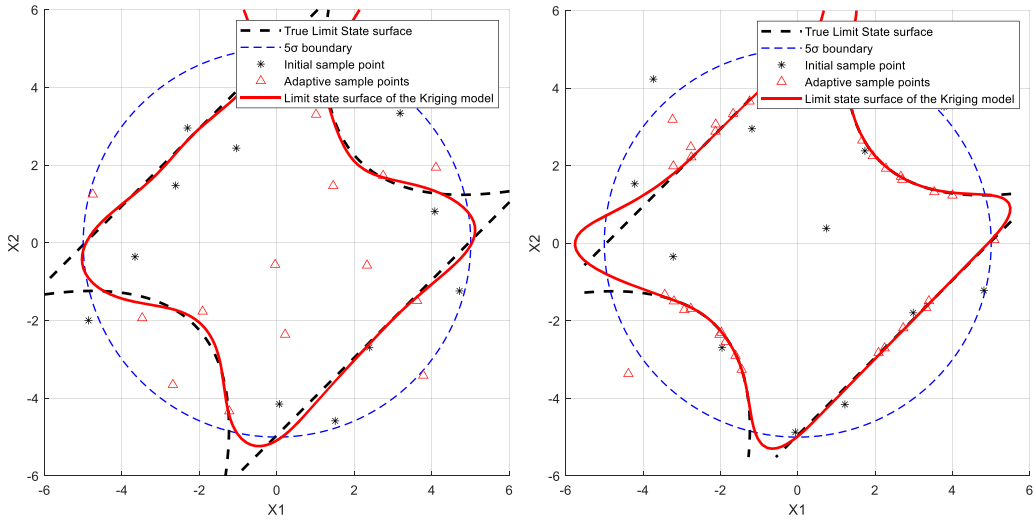

a) AK-MCS-EFF b) AK-MCS-H

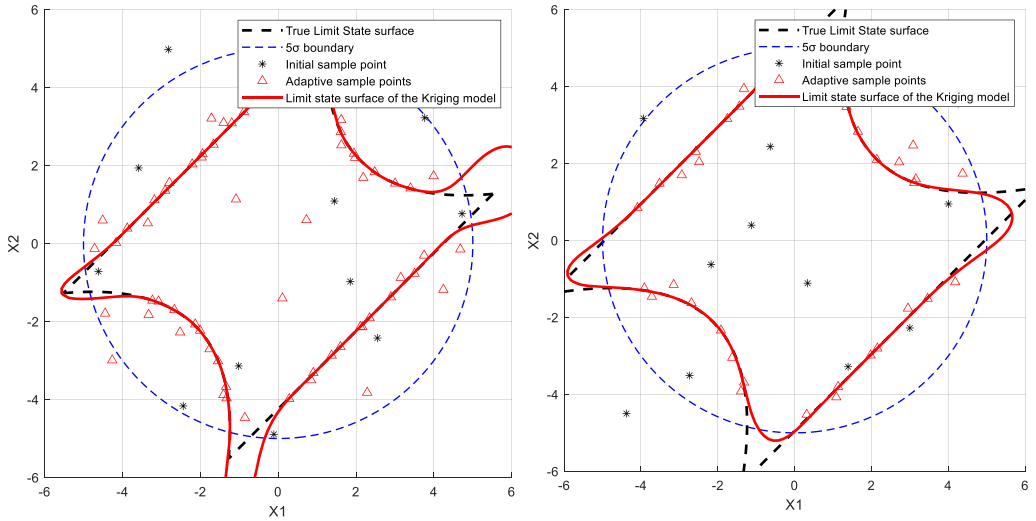

c) AK-MCS- U d) AK-MCS-WU

Figure 7. Modeling results of various methods when $k = 7$.

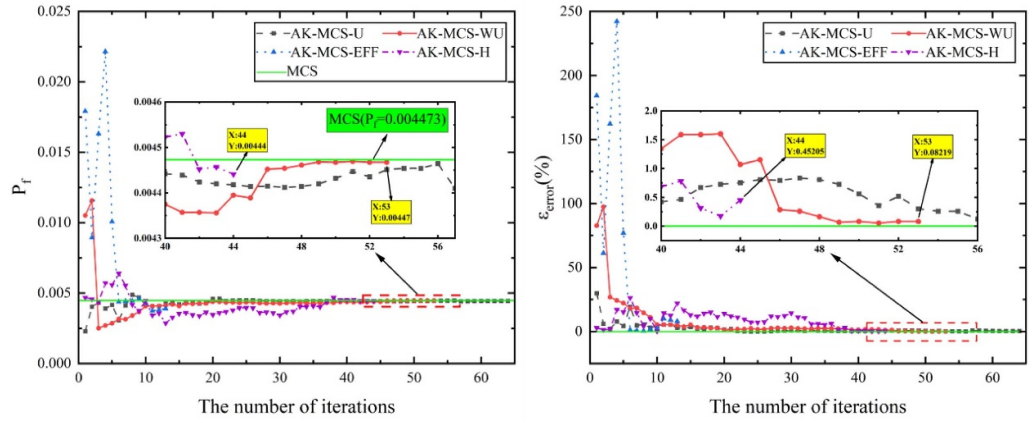

a) Failure probability convergence curve b) Relative error curve

Figure 8. The convergence curve and relative error curve of the failure probability when $k = 6$.

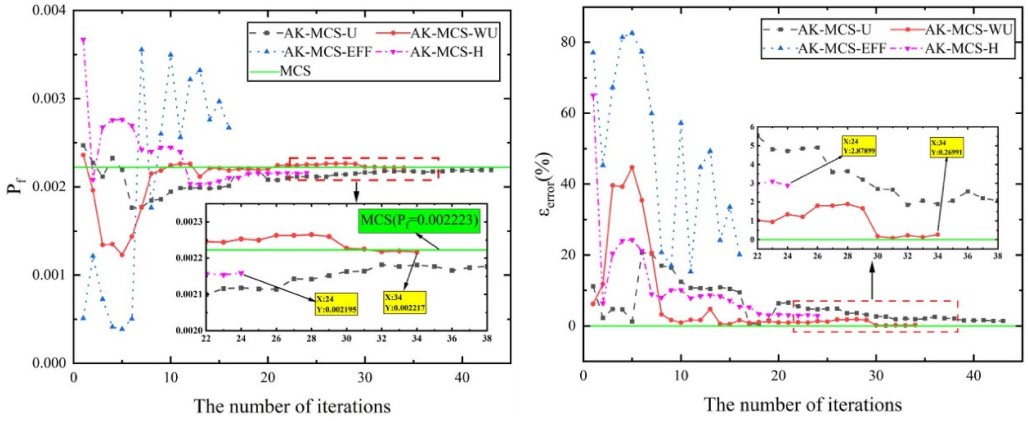

a) Failure probability convergence curve b) Relative error curve

Figure 9. The convergence curve and relative error curve of the failure probability when $k = 7$.

Table 1. The reliability calculation result of Case 1.

k	Method	N_{call}	$P_{\text{f}}/10^{-3}$	$\text{Cov}_{P_{\text{f}}}/\%$	$\varepsilon_{\text{error}}/\%$	T/s
6	MCS	1×10^6	4.473	1.49	—	4.32
	AK-MCS-U	$12 + 59.3$	4.437	1.50	0.80	150.13
	AK-MCS-WU	$12 + 51.1$	4.500	1.49	0.60	143.83
	AK-MCS-EFF	$12 + 14.2$	4.262	1.53	4.7	638.89
	AK-MCS-H	$12 + 32.8$	4.673	1.46	4.5	688.21
7	MCS	1×10^6	2.223	2.12	—	4.13
	AK-MCS-U	$12 + 44.1$	2.192	2.13	1.39	101.30
	AK-MCS-WU	$12 + 37.2$	2.229	2.12	0.27	95.55
	AK-MCS-EFF	$12 + 14.6$	2.271	2.10	2.16	655.91
	AK-MCS-H	$12 + 30.9$	2.116	2.17	4.81	672.66

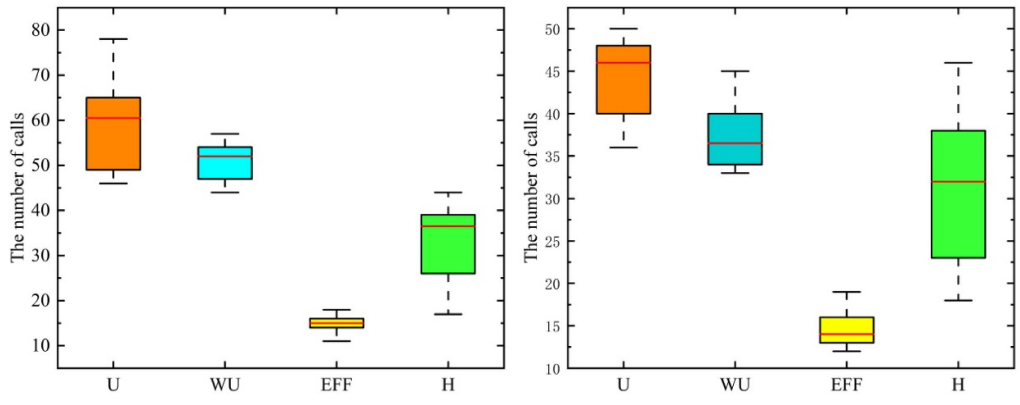

a) k=6 b) k=7

Figure 10. Box plot of the number of times various methods are called to a performance function.

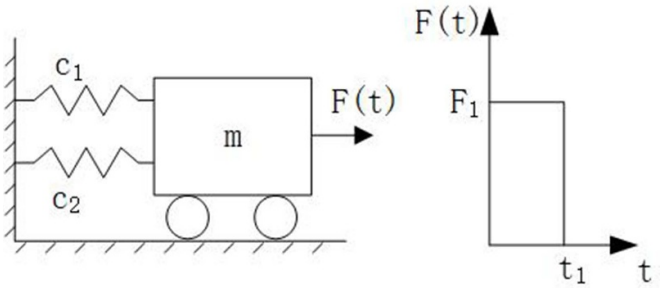

Figure 11. Schematic diagram of a nonlinear oscillator system.

Table 2. Distribution of random variables.

Variable	Distribution	Mean value	Standard deviation
c_1	Normal	1	0.1
c_2	Normal	0.1	0.01
r	Normal	0.5	0.05
F_1	Normal	1	0.2
m	Normal	1	0.05
t_1	Normal	1	0.2

Table 3. The reliability calculation results of Case 2.

Method	N_{call}	$P_{\text{f}}/10^{-2}$	$\text{Cov}_{P_{\text{f}}}/\%$	$\varepsilon_{\text{error}}/\%$	*T*/*s*
MCS	1×10^5	2.859	1.84	—	0.77
AK-MCS-U	12 + 59.4	2.872	1.84	0.45	32.03
AK-MCS-WU	12 + 53.9	2.849	1.85	0.35	27.30
AK-MCS-EFF	12 + 14.2	2.713	1.89	5.1	72.18
AK-MCS-H	12 + 52.9	2.837	1.85	0.77	130.72

Additionally, the box plots of the number of calls to the actual performance function by various methods are shown in figure 12.

In a certain test, the convergence curves of the failure probability and the relative-error curves of various methods are shown in figure 13.

Figures 12 and 13 further prove that although the AK-MCS-EFF method has the fewest calls to the performance function, its relative error in predicting the failure probability is the largest. Compared with the AK-MCS-U method, the AK-MCS-WU method has fewer calls to the performance function, and the relative error of the obtained failure probability can converge well near 0, and the convergence speed is faster.

4.3. Engineering example: structural reliability of ceramic roller

Ceramic rollers play a crucial role in the hot-forming process of high-strength steel by transporting the billets. They are key components of hot-forming equipment, and their performance has a significant impact on the entire hot-forming process and product quality. Ceramic rollers are usually made of high-purity high-temperature ceramic materials such as alumina and silicon carbide to ensure that they have high-temperature resistance, wear resistance, and other properties, enabling them to work stably in a high-temperature environment of up to 1000 °C. The physical model of the ceramic roller drive system is shown in figure 14, which mainly consists of ceramic rollers, iron heads, drive shafts, bearing housings, and sprockets.

Due to the presence of numerous uncertain factors, ceramic rollers may experience failures during operation, which significantly impacts the safety and reliability of hot-forming equipment. This section thoroughly considers the inherent uncertainties in material dimensions, performance, and other parameters. Using finite element simulation technology, the mechanical response of the ceramic roller during the heating process is modeled to obtain response data. Finally, based on the proposed AK-MCS-WU method, the failure probability of the ceramic roller is calculated. Since the solution process involves finite element simulation, which cannot be directly compared with the MCS method, the AK-MCS-U method is used as the control group.

In terms of dimensional parameters, the outer diameter and wall thickness of the ceramic roller directly determine its load-bearing capacity and stress distribution. Regarding material performance parameters, the coefficient of thermal expansion

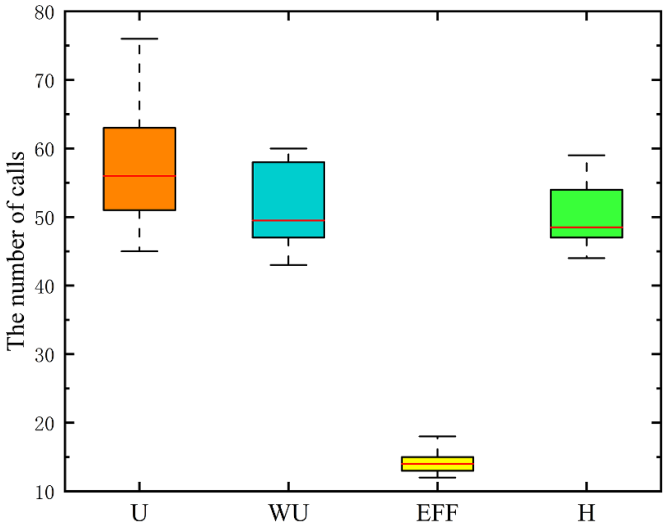

Figure 12. Box plot of the number of times various methods are called to a performance function.

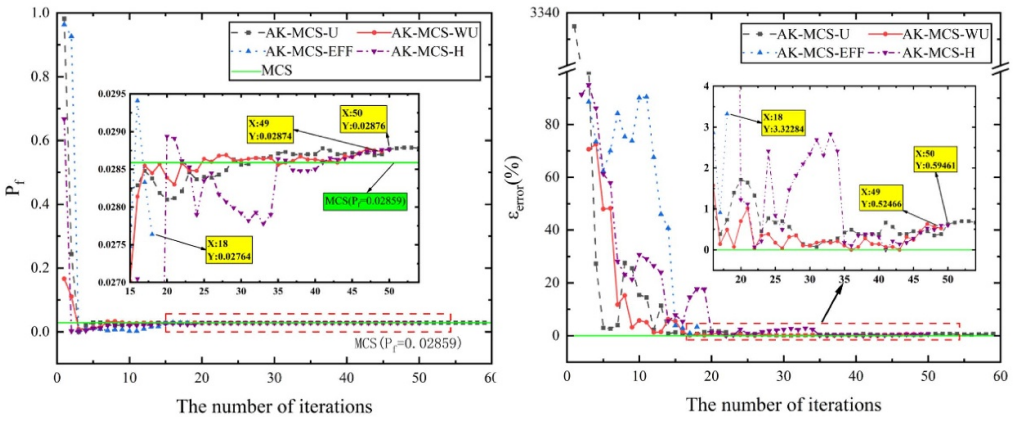

a) Failure probability convergence curve b) Relative error curve

Figure 13. The convergence curve and relative error curve of the failure probability in example 2.

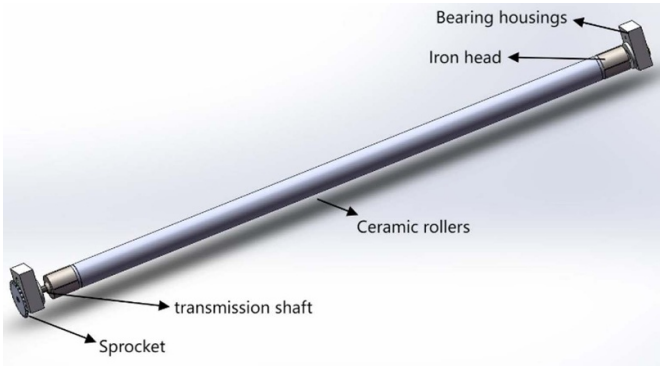

Figure 14. Physical model of a ceramic roller drive system.

is a key indicator for measuring the degree of linear expansion of materials during temperature changes. Its value directly affects the deformation of the roller during variations in the temperature field and plays a crucial role in the generation of thermal stress. Thermal conductivity governs the rate and distribution of heat transfer within the ceramic roller, thereby influencing the uniformity of its internal temperature field and ultimately having an indirect impact on its mechanical properties. Furthermore, parameters such as the elastic modulus and Poisson's ratio are also vital in the static reliability analysis

Table 4. Distribution information of random variables in ceramic rollers.

Variable	Distribution	Mean value	Standard deviation
R (mm)	Normal	80	4
D (mm)	Normal	10	1
α (10^{-6}/°C)	Normal	5	0.5
K W (m*K)$^{-1}$	Normal	2.5	0.2
E (GPa)	Normal	85	5
ν	Normal	0.15	0.05
ρ g cm^3	Normal	3.5	0.4

Table 5. Random parameters and response values.

Test number	Random parameter							Maximum stress (MPa)
	R (mm)	D (mm)	α (10^{-6}/°C)	K W (m*K)−1	E (GPa)	ν	ρ (g/cm^3)	
1	77.61	9.62	5.39	2.38	84.64	0.17	3.23	560.85
2	82.11	7.51	5.43	2.19	88.91	0.19	3.84	554.31
3	82.02	10.44	5.87	2.56	81.85	0.13	3.64	602.40
4	76.71	10.64	3.97	2.51	94.55	0.18	3.49	468.26
5	76.41	11.79	4.94	2.61	89.72	0.13	3.04	524.68
⋮	⋮	⋮	⋮	⋮	⋮	⋮	⋮	⋮
16	78.65	9.39	4.25	2.32	84.17	0.11	2.70	468.26
17	88.75	10.13	5.20	2.80	75.68	0.20	3.29	514.66
18	83.51	9.92	5.57	2.27	79.19	0.17	3.39	589.15
19	81.22	9.22	4.65	2.45	86.66	0.21	3.09	480.79
20	73.64	10.38	5.07	2.72	81.31	0.08	3.73	496.86

of ceramic rollers, as they define the roller's response characteristics under stress. Based on the above analysis, the outer diameter, wall thickness, coefficient of thermal expansion, thermal conductivity, Young's modulus, and Poisson's ratio are set as random variables, denoted by *R, D,* α*, K, E*, and ν, respectively. The distributions and specific parameters of each random variable are shown in table 4.

Since the ceramic roller mainly bears axial compressive stress during the heating process, the axial stress of the ceramic roller is used as the reliability evaluation index, and the performance function of the ceramic roller is established as follows:

$$G(\boldsymbol{X}) = \boldsymbol{\sigma}_{\max}(\boldsymbol{X}) - \boldsymbol{\sigma}_{\mathrm{c}} \tag{35}$$

where X is a random variable, including random variables such as the outer diameter, wall thickness, thermal expansion coefficient, and thermal conductivity of the ceramic roller, $\boldsymbol{X} = (R, D, \alpha, K, E, \upsilon, \rho)^{\mathrm{T}}$; $\sigma_{\max}(\cdot)$ is the actual maximum axial stress of the ceramic roller, obtained through ANSYS simulation; σ_{c} is the critical axial stress of the ceramic roller. By referring to relevant materials, $\sigma_{\mathrm{c}} = 2990\,\mathrm{MPa}$.

A sample space of $N_{\mathrm{MCS}} = 10^6$ is given. The LHS sampling method is used to sample the random input variables of the ceramic roller, and 20 groups of initial sample points are extracted. The ANSYS parametric design language is used to parametrically design the maximum axial stress of the ceramic roller to obtain the maximum axial stress response values of the initial sample points of the ceramic roller. The initial sample points and their response values are shown in table 5. An initial Kriging model is established based on the random variables and the maximum stress response values to form an initial sample set.

The simulation stress contour diagrams of the data in Group 1 and Group 16 in table 5 are shown in figure 15. The maximum stress values are 560.85 MPa and 468.26 MPa respectively.

After constructing the initial Kriging model, the *WU* active learning function is used for the iterative calculation of candidate sample points, and the best sample points are added to the initial sample set. The finite-element simulation is called to obtain the maximum stress response values. The Kriging model is updated by continuously selecting points through the *WU* learning function until the stop criterion is met. Finally, a Kriging model that meets the accuracy requirements is obtained, and the failure probability of the ceramic roller is predicted based on this. The calculation results are shown in table 6, and the convergence curve of the failure probability of a certain test is shown in figure 16.

Under the relevant parameters of the ceramic roller set in this paper, the failure probability of the ceramic roller obtained by the AK-MCS-WU method is 4.874×10^{-4}, which is similar to the calculation result of the AK-MCS-U method. In terms of the number of calls to the finite-element simulation during the calculation process, the AK-MCS-WU method has

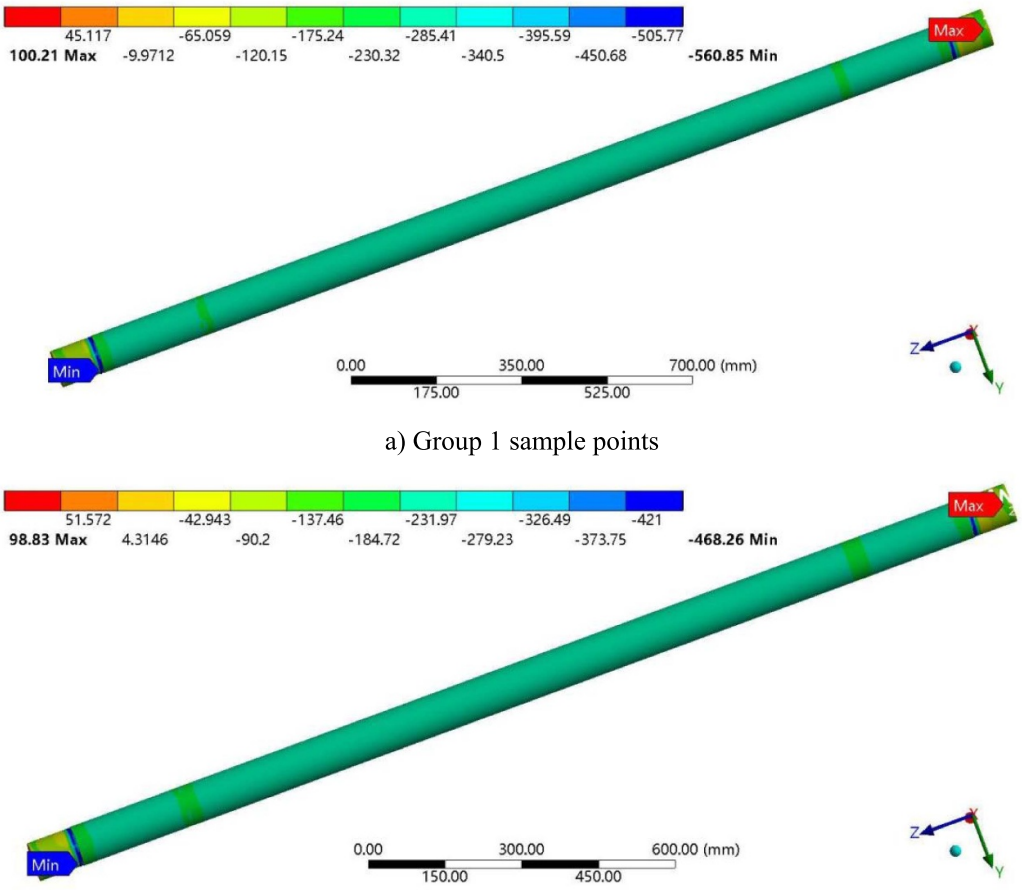

a) Group 1 sample points

b) Group 16 sample points

Figure 15. Initial sample point simulation stress contours.

Table 6. Calculation results of static failure probability of ceramic rollers.

Methon	N_{call}	$P_{\text{f}}/10^{-4}$	$\text{Cov}\left(P_{\text{f}}\right)/\%$
AK-MCS-U	$20+108.2$	4.575	4.54
AK-MCS-WU	$20+96.4$	4.874	4.67

certain advantages and can ensure the stable convergence of the failure probability.

5. Conclusion

Currently, the Kriging model is an important surrogate model for structural reliability analysis. Based on the *U* learning function, the *WU* learning function considers the influence of both the predicted values and the prediction variances of the sample points on the accuracy of failure probability estimation. It prioritizes selecting sample points closer to the LSS in the sample space and assigns a larger weight to the prediction variance of the sample points near the LSS, thereby improving the efficiency of sample point selection. In the process of developing the *WU*-learning function, selecting an appropriate adaptive directional function is crucial. This paper compares the effects of different adaptive directional functions on the selection of sample points by the *WU* learning function. The final chosen adaptive directional function is $\rho_2(x) = 1+\exp(-\left|\mu_{\hat{G}}(x)\right|)$, and based on this, the AK-MCS-WU reliability analysis method is established.

In two numerical examples, although the AK-MCS-EFF and AK-MCS-H methods can effectively reduce the number of calls to the performance function, their relative error in predicting the failure probability is relatively large. Moreover, these two methods require longer average solution times per run, resulting in higher time costs. Compared to the AK-MCS-U method, the AK-MCS-WU method can further reduce the number of calls to the performance function while ensuring

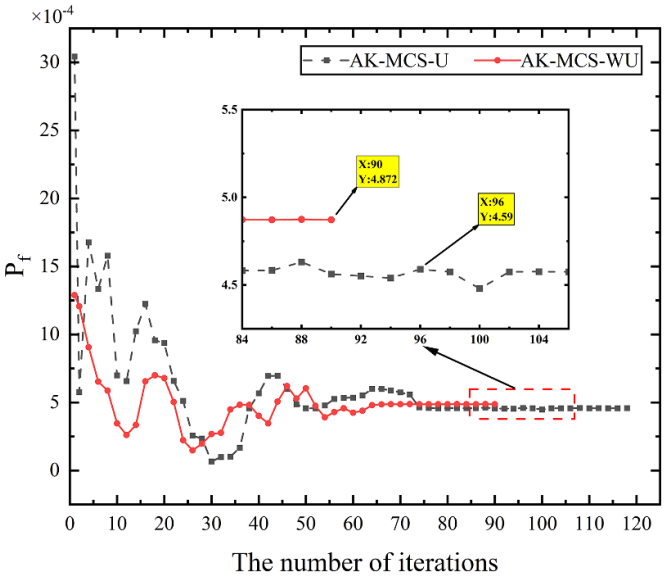

Figure 16. Convergence curve of failure probability of ceramic roller.

the accuracy of failure probability prediction and maintaining lower time costs. Engineering case studies further demonstrate that the AK-MCS-WU method, when applied to reliability problems with complex performance functions, ensures stable convergence of failure probability, reduces the number of calls to the performance function, and offers significant practical value.

The AK-MCS-WU structural reliability analysis method proposed in this paper provides high-accuracy failure probability predictions, but it also has certain limitations. First, compared to the AK-MCS-EFF and AK-MCS-H methods, this approach still requires a relatively large number of calls to the performance function. When dealing with complex finite element simulation models, frequent calls to the finite element simulations result in higher computational costs. Second, the *WU* learning function proposed in this paper has weights that are only related to the predicted values throughout the entire training phase. In future research, we plan to introduce a dynamic weight adjustment mechanism based on training progress. In the early stages of training, the focus will be on enhancing the global search capability of the learning function, encouraging the algorithm to more effectively explore potential multiple failure regions. In the later stages of training, the emphasis will shift to improving its local search capability, allowing for more efficient extraction of local information and accelerating convergence. This approach will comprehensively improve the overall performance of the method.

Acknowledgments

This research was supported by the 2022 industrial technology basic public service platform (No. 2022-232-223-02).

References

[1] Zhao W, Chen Y and Liu J 2020 An effective first order reliability method based on Barzilai–Borwein step *Appl. Math. Modelling* **77** 1545–63

[2] Keshtegar B and Chakraborty S 2018 A hybrid self-adaptive conjugate first order reliability method for robust structural reliability analysis *Appl. Math. Modelling* **53** 319–32

[3] Wang Y, Hao P, Yang H, Wang B and Gao Q 2020 A confidence-based reliability optimization with single loop strategy and second-order reliability method *Comput. Methods Appl. Mech. Eng.* **372** 113436

[4] Meng Z, Zhou H, Hu H and Keshtegar B 2018 Enhanced sequential approximate programming using second order reliability method for accurate and efficient structural reliability-based design optimization *Appl. Math. Modelling* **62** 562–79

[5] Zhu Z and Du X 2016 Reliability analysis with Monte Carlo simulation and dependent Kriging predictions *J. Mech. Des.* **138** 121403

[6] Papaioannou I, Breitung K and Straub D 2018 Reliability sensitivity estimation with sequential importance sampling *Struct. Saf.* **75** 24–34

[7] Xiao S, Oladyshkin S and Nowak W 2020 Reliability analysis with stratified importance sampling based on adaptive Kriging *Reliab. Eng. Syst. Saf.* **197** 106852

[8] Chan J, Papaioannou I and Straub D 2022 An adaptive subset simulation algorithm for system reliability analysis with discontinuous limit states *Reliab. Eng. Syst. Saf.* **225** 108607

[9] Lima J P S, Evangelista F Jr and Soares C G 2023 Hyperparameter-optimized multi-fidelity deep neural network model associated with subset simulation for structural reliability analysis *Reliab. Eng. Syst. Saf.* **239** 109492

[10] Valdebenito M A, Wei P, Song J, Beer M and Broggi M 2021 Failure probability estimation of a class of series systems by multidomain line sampling *Reliab. Eng. Syst. Saf.* **213** 107673

[11] Ameryan A, Ghalehnovi M and Rashki M 2022 AK-SESC: a novel reliability procedure based on the integration of active

learning kriging and sequential space conversion method *Reliab. Eng. Syst. Saf.* **217** 108036
[12] Liu Z and Choe Y 2021 Data-driven sensitivity indices for models with dependent inputs using polynomial chaos expansions *Struct. Saf.* **88** 101984
[13] Zheng S, Jiang A N and Feng K S 2021 A reliability evaluation method for intermittent jointed rock slope based on evolutionary support vector machine *Comput. Model. Eng. Sci.* **129** 149
[14] Hong L, Li H and Peng K 2021 A combined radial basis function and adaptive sequential sampling method for structural reliability analysis *Appl. Math. Modelling* **90** 375–93
[15] Ren C, Aoues Y, Lemosse D and De Cursi E S 2022 Ensemble of surrogates combining Kriging and artificial neural networks for reliability analysis with local goodness measurement *Struct. Saf.* **96** 102186
[16] El Haj A-K and Soubra A-H 2021 Improved active learning probabilistic approach for the computation of failure probability *Struct. Saf.* **88** 102011
[17] Ma Y-Z, Jin X-X, Wu X-L, Xu C, Li H-S and Zhao Z-Z 2023 Reliability-based design optimization using adaptive Kriging-A single-loop strategy and a double-loop one *Reliab. Eng. Syst. Saf.* **237** 109386
[18] Krige D G 1951 A statistical approach to some basic mine valuation problems on the Witwatersrand *J. South. Afr. Inst. Min. Metall.* **52** 119–39
[19] Matheron G 1963 Principles of geostatistics *Econ. Geol.* **58** 1246–66
[20] Lophaven S N, Nielsen H B and Søndergaard J 2002 DACE-A matlab Kriging toolbox version 2.0
[21] Kaymaz I 2005 Application of kriging method to structural reliability problems *Struct. Saf.* **27** 133–51
[22] Echard B, Gayton N and Lemaire M 2011 AK-MCS: an active learning reliability method combining Kriging and Monte Carlo simulation *Struct. Saf.* **33** 145–54
[23] Huang X, Chen J and Zhu H 2016 Assessing small failure probabilities by AK–SS: an active learning method combining Kriging and subset simulation *Struct. Saf.* **59** 86–95
[24] Echard B, Gayton N, Lemaire M and Relun N 2013 A combined importance sampling and kriging reliability method for small failure probabilities with time-demanding numerical models *Reliab. Eng. Syst. Saf.* **111** 232–40
[25] Bichon B J, Eldred M S, Swiler L P, Mahadevan S and McFarland J M 2008 Efficient global reliability analysis for nonlinear implicit performance functions *AIAA J.* **46** 2459–68
[26] Lv Z, Lu Z and Wang P 2015 A new learning function for Kriging and its applications to solve reliability problems in engineering *Comput. Math. Appl.* **70** 1182–97
[27] Zhang X, Wang L and Sørensen J D 2019 REIF: a novel active-learning function toward adaptive Kriging surrogate models for structural reliability analysis *Reliab. Eng. Syst. Saf.* **185** 440–54
[28] Shi Y, Lu Z, He R, Zhou Y and Chen S 2020 A novel learning function based on Kriging for reliability analysis *Reliab. Eng. Syst. Saf.* **198** 106857
[29] Yang X, Liu Y, Gao Y, Zhang Y and Gao Z 2015 An active learning kriging model for hybrid reliability analysis with both random and interval variables *Struct. Multidiscip. Optim.* **51** 1003–16
[30] Sun Z, Wang J, Li R and Tong C 2017 LIF: a new Kriging based learning function and its application to structural reliability analysis *Reliab. Eng. Syst. Saf.* **157** 152–65
[31] Wang Z and Shafieezadeh A 2019 ESC: an efficient error-based stopping criterion for kriging-based reliability analysis methods *Struct. Multidiscip. Optim.* **59** 1621–37
[32] Zhang Y, Dong Y and Xu J 2023 An accelerated active learning Kriging model with the distance-based subdomain and a new stopping criterion for reliability analysis *Reliab. Eng. Syst. Saf.* **231** 109034
[33] Peijuan Z, Ming W C, Zhouhong Z and Liqi W 2017 A new active learning method based on the learning function U of the AK-MCS reliability analysis method *Eng. Struct.* **148** 185–94
[34] Meng Y, Zhang D, Shi B, Wang D and Wang F 2024 An active learning Kriging model with approximating parallel strategy for structural reliability analysis *Reliab. Eng. Syst. Saf.* **247** 110098
[35] Cao R N, Sun Z L, Zhang Y B and Wang J 2020 Reliability analysis based on active learning for complex mechanical structure *J. Northeastern Univ.* **41** 223

Hongyan Chu received the Ph.D. degree in mechanical design and theory from Beijing University of Technology, Beijing, China, in 2003. She is currently a professor of the Beijing Key Laboratory of Design and Intelligent Machining Technology for High Precision Machine Tools, Beijing University of Technology. She has published more than 40 SCI/EI papers. Her research interests include reliability and accuracy retention of manufacturing equipment, intelligent manufacturing technology, and optimization algorithm.

Wenzhong Li received a bachelor's degree from Beijing University of Technology (Beijing, China) in 2018. He is currently pursuing a master's degree at the College of Mechanical and Energy Engineering, Beijing University of Technology (Beijing, China). His main research interests are the innovation and application of reliability analysis methods.

Dongyang Sun received his master's degree from Beijing University of Technology (Beijing, China) in 2019. He is currently pursuing his doctor's degree at the College of Mechanical and Energy Engineering, Beijing University of Technology (Beijing, China). His research interests include vacuum furnace reliability design and evaluation.

Zhifeng Liu received the Ph.D. degree in mechanical design from the Mechanical Engineering and Automation College, Northeastern University, in 2001. He is currently a professor of Key Laboratory of CNC Equipment Reliability, Ministry of Education, School of Mechanical and Aerospace Engineering, Jilin University; and a distinguished Professor of Institute of Advanced Manufacturing and Intelligent Technology, Beijing University of Technology. His research interests include robotic motion control, machine vision technology, networked manufacturing, and manufacturing system information.

Weixu Zheng is a postgraduate student at Beijing University of Technology. His research interests include time-variant reliability and reliability prediction.

Jingjing Xu received the Ph.D. degree in mechanical engineering from the Beijing University of Technology, in 2020. She is currently a Lecturer with the Institute of Advanced Manufacturing and Intelligent Technology, Faculty of Materials and Manufacturing, Beijing University of Technology. Her research interests include the robotic control and arms coordination. She has made some progress in the studying on kinematic analysis and motion control of redundant manipulators.

Qiang Cheng received the Ph.D. degree from Huazhong University of Science and Technology in 2009. He currently serves as a professor and Ph.D. supervisor at Beijing University of Technology. He has published more than 100 SCI papers and been authorized with over 80 invention patents in the UK, Japan, and China. His main research interests include high-end manufacturing equipment, intelligent manufacturing, and medical robots.